Estimating the Error in Calculated Deflections of HPC Slabs: A Parametric Study Using the Theory of Error Propagation

Mahmoud M. Reda Taha and Mostafa A. Hassanain

Synopsis:

Although limit state design blends both serviceability and strength limit states, most engineers tend to be less confident in serviceability limit states than in strength limit states, especially when deflections of reinforced concrete slabs are considered. A major source of this lack of confidence is the existence of many uncertain variables in calculating slab deflections such as concrete properties (e.g., modulus of elasticity, modulus of rupture), creep coefficient, curing regime and duration, and the existence of construction loads. The absence of any reliability coefficients in deflection calculations or deflection limits gives the impression that engineers are expected to evaluate the exact deflection that will take place on site.

To make matters worse, the introduction of high-performance concrete (HPC) has increased the uncertainty about concrete properties. While HPC enhances the overall material's performance, it is usually reported to have higher shrinkage strains, and it is more susceptible to plastic shrinkage than normal-strength concrete (NSC). The possible reduction of curing periods from the recommended one week to two or three days due to tight construction schedules can result in substantial microcracking which would significantly reduce the concrete modulus of rupture. Therefore, serviceability performance is dependent on many inter-related factors that the engineer cannot control in the design assumptions. Unless the band of errors in deflection calculations is known to the engineer, the lack of confidence in deflection calculations will always be there.

This paper describes a mathematical model utilizing the theory of error propagation to predict the error in the calculated deflections of simply-supported, one-way reinforced concrete slabs. Parametric studies have been carried out to examine the effect of changing the concrete properties as a result of changed site conditions on the accuracy of the estimated deflections.

ACI member Mahmoud M. Reda Taha, Ph.D., P.Eng. is a structural engineer at Stantec Consulting Ltd., Calgary, Canada. He is a member of ACI Committee 440 (Fibre Reinforced Polymers-FRP) and 548 (Polymers in Concrete). His research interests include reinforced and prestressed concrete structures, computer applications in structural design, fracture mechanics, and use of FRP in structures.

ACI member Mostafa A. Hassanain, Ph.D., P.Eng. is a structural engineer at Edwards and Kelcey, Inc., Minneapolis, Minnesota. He is an associate member of Joint ACI-ASCE Committee 343 (Concrete Bridge Design). His research interests include behaviour and design of reinforced concrete structures, computer-aided analysis and design of prestressed concrete bridges, and structural optimization.

INTRODUCTION

The majority of building design codes accepts Branson's approach (1) as the basis for calculating a reduced concrete stiffness for a cracked concrete section that can be used in elastic analysis to estimate the immediate deflection. This reduced stiffness is represented by an effective moment of inertia, I_e, not greater than I_g, the moment of inertia of the gross concrete section about its centroidal axis neglecting reinforcement. Both the American Code ACI 318-99 (2) and the Canadian Code CSA A23.3-M94 (3) utilize this approach, as represented by Eq. [1]

$$I_e = I_{cr} + (I_g - I_{cr})\left(\frac{M_{cr}}{M_a}\right)^3 \leq I_g \qquad [1]$$

where I_{cr} is the moment of inertia of a cracked section transformed to concrete, neglecting concrete in tension; M_{cr} is the cracking moment as given by Eq. [2]; and M_a is the maximum moment in a member at the load stage deflection is calculated.

$$M_{cr} = \frac{f_r I_g}{y_t} \qquad [2]$$

f_r is the modulus of rupture of concrete; and y_t is the distance from the centroidal axis of gross section to the extreme fibre in tension. When Eq. [1] is used, design codes allow the designer to estimate the additional long-term deflection resulting from creep and shrinkage by multiplying the immediate deflection due to sustained load by a simple multiplier, ζ, given by

$$\zeta = \frac{S}{1 + 50\,\rho'} \qquad [3]$$

where S is a time-dependent factor equal to 2.0, 1.4, 1.2, and 1.0, respectively, for 5 years or more, 12 months, 6 months, and 3 months; ρ' ($= A_s'/bd$) is the ratio of compression reinforcement at mid-span for a simple span; A_s' is the area of compression reinforcement; b is the width of compression face of member; and d is the distance from the extreme compression fibre to the centroid of tension reinforcement.

Sherif and Dilger (4), Ghali and Azarnejad (5), and Gilbert (6) criticized the use of Eq. [1] showing that if the actual moment M_a in a concrete slab is close to the cracking capacity of the slab, M_{cr}, this equation would indicate that the value of I_e is close to I_g when in reality the slab has already cracked. While neglecting the tension stiffening effect in a cracked concrete section would have a negligible effect on the estimated deflection in cases where the total moment M_a is three to four times larger than M_{cr}, it would have a significant effect if M_a is between one and two times M_{cr} (5).

Time-dependent deformations of concrete members depend on many factors including the properties of concrete, geometry of the member, and ambient conditions such as temperature and relative humidity. The use of a single multiplier (Eq. [3]) that is dependent only on time and the amount of compression reinforcement cannot possibly account for all of these factors, and therefore, cannot yield consistent and accurate values for the deflection (5,6,7).

The mean curvature method is a more accurate and more general method for predicting deflections of concrete members. It has been adopted by the CEB-FIP Model Code 90 (MC-90) (8). In this method, the deflection of a member can be determined from the values of the curvature Ψ at a number of sections (9). For example, the deflection at mid-span of a simply-supported, one-way slab using three sections along the span with parabolic variation of Ψ between them is determined by double integration of the curvature along the span (9). The mid-span deflection, Δ_{Mid}, can be given by the geometrical relationship

$$\Delta_{Mid} = \frac{L^2}{96}\left(\Psi_{Left} + 10\Psi_{Mid} + \Psi_{Right}\right) \qquad [4]$$

where

$$\Psi_i = \frac{M_i}{E_c I_{ei}} \qquad [5]$$

where L is the span length; M is the bending moment; and E_c is the modulus of elasticity of concrete. Increasing the number of sections will increase accuracy. Equations to estimate the deflection based on the calculated curvature at various sections along the member with different end conditions are given by Ghali and Favre (9). The mean curvature method accounts for the variation in cross-

sectional properties (i.e., the loss of stiffness) that inevitably occurs with time in concrete members due to cracking.

SOURCES OF ERROR IN DEFLECTION CALCULATION

Jokinen and Scanlon (10) analyzed several field measurements on identical slabs in a multi-story building. They reported a coefficient of variation between calculated and measured deflections in the range of 30 percent for both short and long-term deflections. However, a recent study conducted by Ghali *et al*. (11) to monitor the deformations of the Confederation Bridge in Canada showed the variation between the measured and the predicted values to be very small when the recorded concrete properties rather than the predicted ones were used. Such observations raise the concern that error accumulation in deflection calculations can have a significant effect on the predicted deflection values.

Three sources of errors affect the accuracy of the calculated deflections in reinforced concrete members; these are computational errors, methodological errors and, errors due to uncertainties. Computational errors are usually referred to as human errors and they can happen during computations. In his review of computational errors, Fling (12) showed that the current method of calculating deflections includes ten steps of computations of the load, moment, location of centroid of the gross concrete cross section, gross uncracked moment of inertia, section modulus of gross cross section, cracking moment, cracked moment of inertia, effective moment of inertia, instantaneous deflection, and long-term deflection. If the probability of error in each step is between 1 and 2 percent, the final deflection will deviate by 10 to 20 percent from its correct value. The use of computers minimizes the probability of computational errors.

The second source of errors is related to the use of simplified versus detailed analysis. Although it is not expected that engineers will use detailed analysis to estimate deflections in all cases, the degree by which the accuracy of the calculation is jeopardized when specific assumptions are made, should be taken into account when final deflections are evaluated and compared to standard limits.

The third source of errors is related to the uncertainties in the parameters included in deflection computations, specifically the loading values and history, and the concrete properties. Gardner (13) showed that neglecting construction loads and/or construction schedule could result in excessive deflection of two-way concrete slabs. Fling (12) showed that while some of these parameters are known before construction, a considerable number, including concrete properties, may be uncertain until construction takes place. Not only are concrete properties not known before construction, but also those properties incorporated in deflection calculation (i.e., modulus of elasticity, modulus of rupture, and time-dependent

parameters) have wide scatter in their values. Concrete properties affect the predicted deflection both directly by affecting the structural stiffness of the element, and indirectly by defining the way moment distribution and redistribution takes place in the structural system. The focus of this study is on examining the effect of the uncertainties of concrete properties on the accuracy of the predicted deflections.

Application of probabilistic concepts to serviceability computations has been rarely addressed (14,15). Zundelevich *et al*. (16) applied the principles of error propagation to predict the variation in the final deflection of prestressed concrete elements using separate measures of the elastic and the long-term deflections at different loading stages. The study showed that a measured variation of 12 percent in time-dependent deflection resulted in a 10 percent variation in the total deflection. Thompson and Scanlon (17) noted that code deflection computations would only provide an estimate of the mean deflection. The probability to exceed this mean deflection would be about 50 percent if normal distribution of slab deflection is assumed. Scanlon and Pinheiro (18) compared the current deterministic approach to deflection control to a probabilistic approach for design for safety. They suggested that the best practical probability limit can be generated using a measure of the associated damage to serviceability due to excessive deflections.

CONCRETE PROPERTIES: MODELS AND UNCERTAINTIES

Modulus of Rupture

The modulus of rupture, f_r, is a measure of the tensile strength of concrete under pure flexural stresses. Most design codes have adopted the modulus of rupture as a representative of concrete cracking strength in deflection computations. Design codes provide different prediction models for the modulus of rupture. Most of these models relate the modulus of rupture to the square root of the concrete compressive strength, f_c', in order to reflect the disproportional increase of the modulus of rupture with respect to the increase in the compressive strength.

Equations [6] to [11] give the models to predict the modulus of rupture of concrete in MPa as per ACI 318-99 metric and U.S. customary units editions (2), CSA A23.3-M94 (3), Standards New Zealand NZS 3101 (19), Standards Australia AS 3600-1994 (20), and the Ontario Highway Bridge Design Code (OHBDC) (21), respectively. Figure 1 shows the variation in the modulus of rupture of concrete with respect to its compressive strength for the different design codes. It is worth mentioning that CSA A23.3-M94 (3) requires the reduction of the value of f_r to half of the value given by Eq. [8] when deflection of

two-way slabs is computed. This reduction is considered to account for the effect of cracking due to restrained shrinkage of two-way slabs based on the work of Thompson and Scanlon (17).

$$f_r = 0.7\sqrt{f_c'} \qquad \text{ACI 318-99 metric (2)} \qquad [6]$$

$$f_r = 0.62\sqrt{f_c'} \qquad \text{ACI 318-99 U.S. (2)} \qquad [7]$$

$$f_r = 0.6\sqrt{f_c'} \qquad \text{CSA A23.3-M94 (3)} \qquad [8]$$

$$f_r = 0.6\sqrt{f_c'} \qquad \text{NZS 3101 (19)} \qquad [9]$$

$$f_r = 0.6\sqrt{f_c'} \qquad \text{AS 3600-1994 (20)} \qquad [10]$$

$$f_r = 0.5\sqrt{f_c'} \qquad \text{OHBDC (21)} \qquad [11]$$

CEB-FIP MC-90 (8) and the new Canadian Highway Bridge Design Code (CHBDC) (22) are the only codes to abandon the modulus of rupture as a criterion for cracking of concrete. While CEB-FIP MC-90 (8) uses the mean tensile strength to represent the limit of tensile strength of concrete, CHBDC (22) adopts a new term called the cracking strength to represent the stress level at which concrete cracks. The use of a reduced value to represent cracking is intended to reflect the uncertainty in concrete cracking strength because of its significant variation with shrinkage and thermal strains developed in the section (23). Equations [12] and [13] give the concrete tensile / cracking strength adopted by CEB-FIP MC-90 (8) and CHBDC (22), respectively for use in estimating deflections.

$$f_t = 1.4\left(\frac{f_c'}{10}\right)^{2/3} \qquad \text{CEB-FIP MC-90 (8)} \qquad [12]$$

$$f_{crack} = 0.4\sqrt{f_c'} \qquad \text{CHBDC (22)} \qquad [13]$$

It has been suggested that most of the models developed to predict the modulus of rupture of concrete based on its compressive strength are inaccurate (24,25). Raphael (25) was the first to propose abandoning the square root models for predicting the modulus of rupture of concrete based on its compressive strength. He proposed the following expression

$$f_r = 0.7 \left(f_c'\right)^{2/3} \quad [14]$$

Recent attempts to predict the concrete splitting tensile strength and its modulus of rupture using the compressive strength have been reported by Oluokun (26), and Légeron and Paultre (27). They revealed similar trends presented in Eqs. [15] and [16], respectively. It is worth mentioning that the only code that does not use the square root model is CEB-FIP-MC90 (8).

$$f_t = 0.214 \left(f_c'\right)^{0.69} \quad [15]$$

$$f_r = 0.5 \left(f_c'\right)^{2/3} \quad [16]$$

As it has been established that these two models have much lower coefficients of variation than those models using the square root of f_c', it seems that the insistence on using the square root of f_c' to predict the tensile strength generally, and the modulus of rupture specifically hinders the attempts to develop more accurate prediction models. Figure 2 compares these two models for predicting the modulus of rupture of concrete using Eqs. [15] and [16]. The variation between the predicted modulus of rupture from these equations is still in the range of ± 15 percent.

Modulus of Elasticity

Design codes provide prediction models for the modulus of elasticity of concrete, E_c, based on its f_c'. Equations [17] to [23] give the models to predict E_c in MPa as per ACI 318-99 metric and U.S. customary units editions (2), CSA A23.3-M94 (3), NZS 3101 (19), AS 3600-1994 (20), OHBDC (21), and CEB-FIP MC-90 (8), respectively. While AS 3600-1994 (20) explicitly states that the predicted value may include a variation of ± 20 percent, no other standard indicates how much variation to be expected in the predicted value of E_c.

$$E_c = 4700 \sqrt{f_c'} \quad \text{ACI 318-99 metric (2)} \quad [17]$$

$$E_c = 4730 \sqrt{f_c'} \quad \text{ACI 318-99 U.S. (2)} \quad [18]$$

$$E_c = 4500 \sqrt{f_c'} \quad \text{CSA A23.3-M94 (3)} \quad [19]$$

$$E_c = 4700 \sqrt{f_c'} \quad \text{NZS 3101 (19)} \quad [20]$$

$$E_c = \gamma^{1.5} (0.043 \sqrt{f_c'}) \quad \text{AS 3600-1994 (20)} \quad [21]$$

$$E_c = 5000 \sqrt{f_c'} \quad \text{OHBDC (21)} \quad [22]$$

$$E_c = 21500 \ \kappa \left(\frac{f_c'}{10} \right)^{1/3} \quad \text{CEB-FIP MC-90 (8)} \quad [23]$$

where γ in Eq. [21] is the concrete density (in kg/m^3), and κ in Eq. [23] is a parameter that equals 0.85 to account for the initial plasticity of concrete when elastic analysis of the structure is to be performed. Figure 3 shows the variation in the modulus of elasticity of concrete with respect to its compressive strength for the different design codes. For concrete strengths from 20 MPa to 80 MPa, there exists a difference in the predicted modulus of elasticity in the range of 4.3 percent, 7.6 percent, and an average of 10 percent between ACI 318-99 metric (2), and CSA A23.3-M94 (3), AS 3600-1994 (20), and CEB–FIP MC-90 (8), respectively. It is worth mentioning that the difference between the two Canadian standards, CSA A23.3-M94 (3) and OHBDC (21) is ± 10 percent.

Creep and Shrinkage

Several methods in the form of charts and/or mathematical expressions are provided by different design codes to estimate the expected creep coefficient, ϕ_c, and shrinkage strain, ε_{sh}. However, it is widely accepted that the predicted creep and shrinkage parameters would incorporate large variations (28). The effect of creep and the effect of shrinkage of concrete on deflections have been proved to be interdependent (29). However, they are normally separated during computations. Restrained shrinkage produces internal tensile stress, f_{sh}, which detracts from the cracking and the tension stiffening capacities of the concrete section (6,30). The effect of shrinkage on the cracking capacity of concrete is represented by Eq. [24].

$$f_{cr} = f_r - f_{sh} \quad [24]$$

where f_{cr} is the cracking strength of concrete. The stress f_{sh} can be evaluated using the following expression suggested by Gilbert (6).

$$f_{sh} = \left(\frac{3.5 \ \rho \ (1 + 0.8 \ \phi_c \ ) \ E_s}{E_c + 3 \ \rho \ (1 + 0.8 \ \phi_c \ ) \ E_s} \right) E_a \ \varepsilon_{sh} \quad [25]$$

where

$$\rho = \frac{A_s}{b\,d} \qquad [26]$$

A_s is the area of tension reinforcement; E_s is the modulus of elasticity of steel; and E_a is the age-adjusted modulus of elasticity of concrete that takes into account the reduction in concrete stiffness with time due to the effect of creep. Thus, E_a is a function of the creep coefficient as follows

$$E_a = \frac{E_c}{1 + 0.8\,\phi_c} \qquad [27]$$

Shrinkage also affects the deflection by inducing a curvature, Ψ_{sc}, of the slab when unequal tension reinforcement and compression reinforcement areas are used (6,31). This curvature can be approximated using Eq. [28] (6).

$$\Psi_{sc} = \Gamma \frac{\varepsilon_{sh}}{h}\left(1 - \frac{A_s{}'}{A_s}\right) \qquad [28]$$

The factor Γ is taken as 0.7 for uncracked and 1.2 for cracked sections, respectively; and h is the overall depth of the member.

The effect of creep is considered in calculating both the shrinkage stress as shown in Eq. [25], and in increasing the curvature induced by the sustained load as shown in Eq. [29] (6).

$$\Psi_t = \Psi_i\left(1 + \frac{\phi_c}{\alpha}\right) \qquad [29]$$

where Ψ_t is the long-term curvature at any time t due to a sustained service moment; Ψ_i is the initial curvature due to the sustained service moment; and α is a term that accounts for the effect of cracking and the braking action of the reinforcement, and is a function of the tension and compression reinforcement ratios. Gilbert (6) provided simplified expressions for α for uncracked and cracked cross sections. The effect of creep and shrinkage can be incorporated in a more detailed analysis using the transformed section method proposed by Ghali and Favre (9). It is worthy mentioning that shrinkage stresses less than those estimated using Eq. [25] would be predicted if the transformed section method is used.

Based on this review, it can be concluded that the value of the modulus of rupture specified in most design codes is a best guess rather than a fixed material property. In addition, it can be seen that there is a large variation in the predicted value of the modulus of elasticity. Because both creep and shrinkage

fundamentally affect the concrete stiffness and cracking capacity, it is possible to consider the errors in ϕ_c and ε_{sh} to be incorporated in the errors assumed in the modulus of elasticity and the modulus of rupture, respectively. Therefore, even with the best construction procedures, the estimated modulus of rupture or modulus of elasticity using code equations would probably have an error of ± 30 percent.

UNCERTAINTIES WITH HIGH-PERFORMANCE CONCRETE

Several definitions of high-performance concrete (HPC) exist that are mostly dependent upon the production capacities and practices at different locations. The American Concrete Institute broadly defines HPC as concrete that meets special performance and uniformity requirements that cannot always be achieved routinely using conventional ingredients, normal mixing and placing procedures, and typical curing practices (32). These requirements may involve enhancements of placement and compaction without segregation, long-term mechanical properties, early-age strength, toughness, volume stability, and service-life in severe environments. These stringent quality control measures should theoretically reduce the coefficients of variation of HPC properties compared to those of normal-strength concrete (NSC) properties. However, experience has shown that some HPC properties are highly dependent on curing conditions. Unless an efficient curing regime is adopted, the coefficients of variation of HPC properties that are affected by microcracking (e.g., tensile strength) will be higher than those of NSC.

Research work proved that the modulus of rupture of concrete specimens cured under standard testing conditions, and the modulus of rupture of specimens cured under site conditions differ significantly. These differences varied between 18 percent to 30 percent for NSC (24), and 35 percent to 100 percent for HPC (27). Légeron and Paultre (27) proposed a mathematical model relating the real modulus of rupture, $f_{r\text{-}real}$, to the modulus of rupture determined under standard condition, f_r, as shown in Eq. [30].

$$f_{r-real} = \left(\frac{1}{1.09 + 0.0034\, f_c^{'}} \right) f_r \qquad [30]$$

The best curing regime for HPC is seven days of wet curing followed by dry curing. Due to tight construction schedules, these requirements are hardly met in most situations, despite the widely known adverse effects on the performance of HPC when inadequate curing is practiced (33,34). HPC is more susceptible to shrinkage cracks than NSC. In addition, shrinkage cracks of HPC are more harmful to the modulus of rupture than they are in NSC. Raphael (25), and Légeron and Paultre (27) showed how the moisture gradient due to drying induces

tensile stresses at the concrete surface causing microcracks to develop, and therefore reducing the modulus of rupture of NSC when it is improperly cured. Although this behaviour applies to HPC, it only constitutes part of the picture. The tensile stresses due to drying at the surfaces of HPC members are expected to be higher than in NSC members due to the significant increase of the cementitious material content (e.g., Portland cement, slag, silica fume, and/or fly ash). In addition, the increased autogenous shrinkage of HPC is expected to cause homogeneous tensile shrinkage strains in the whole member mass if shrinkage is restrained. Thus, several microcracks can develop in the whole HPC member if not properly cured rather than at the skin only as in the case of NSC.

Application of fracture mechanics principles to concrete show that the existence of microcracks in the tension zone of a concrete member would significantly reduce the modulus of rupture, but would not have a significant effect on the compressive strength (35). This explains why curing has a more significant effect on the modulus of rupture of HPC than on that of NSC, and why a wide scatter should be expected and accounted for when the modulus of rupture of HPC is being determined. It also explains why it is more difficult to link the modulus of rupture of HPC to its compressive strength, as both properties are not affected by the same factors in a similar manner. It is therefore recommended to measure the modulus of rupture of HPC when needed rather than using irrelevant models to predict it (33).

HPC has a higher elastic modulus and a more brittle post-peak behaviour than NSC. HPC also responds to elastic stresses in a different manner than NSC. The weak aggregate/cement paste transition zone in NSC allows the cement paste to dominate the response to stresses within the elastic range. In HPC, the transition zone is much stronger than in NSC, and failure usually occurs within the aggregate particles. Therefore, more stress transfer to the aggregate takes place within the elastic range, and the aggregate shares a relatively large portion of the elastic response (33). Baalabaki *et al*. (36) proved the possibility of producing two HPC mixes with the same compressive strength and very different moduli of elasticity. Thus, when HPC is used, the above models are not valid, and their prediction of the modulus of elasticity is not accurate.

Research work revealed that HPC would have higher total shrinkage strains and lower creep coefficients than NSC due to its low water/cementitious materials ratio (33). Therefore, a reduction of curing periods, as discussed earlier, would significantly affect the shrinkage and creep performance of HPC. Dilger and Wang (37) showed that creep and shrinkage models for NSC cannot be used for HPC. This is because of the different proportions between basic and drying creep, and autogenous and drying shrinkage in HPC compared to NSC. Few design codes have adopted models for predicting creep and shrinkage of HPC (e.g., The French Code) (AFREM) (38).

APPLICATION OF THE THEORY OF ERROR PROPAGATION TO DEFLECTION COMPUTATION

It is assumed herein that the variation in concrete properties (i.e., modulus of elasticity and modulus of rupture) is the only source of error in deflection calculations. All other factors including ambient conditions, loading conditions, and time-dependent parameters are assumed either to have no errors, or to have their errors incorporated in the errors of the modulus of elasticity and the modulus of rupture. The large number of factors affecting the final deflection of a slab makes it prohibitive to consider all of them simultaneously. An extensive research program would be required to examine all of these factors separately, and a more sophisticated technique than the direct application of the theory of error propagation would be needed to examine their interaction. It is important to emphasize that the principles applied below are applicable to both HPC and NSC. However, HPC might have higher variations in its modulus of rupture because of its higher susceptibility to microcracking.

To examine the effect of the variation of concrete properties on the accuracy of calculated deflections of slabs, a method of deflection prediction should be selected. The theory of error propagation (39) would then be applied to the selected method to derive the expected error in the final deflection value based on the errors incorporated in its parameters. The method selected here for predicting deflections is the mean curvature method (Eq. [5]). Interpolation between the uncracked and cracked section stiffnesses is performed using Branson's approach (Eq. [1]). Combining these two approaches would provide a rational method for predicting deflections, while keeping the method utilized by most design codes to estimate member stiffness. Time-dependent parameters are incorporated by using Eqs. [24] to [29].

The general form of error propagation for a variable z that is a function of two variables x and y is presented in Eqs. [31] through [33].

$$z = f(x, y) \qquad [31]$$

$$\sigma_z^2 = \sigma_x^2 \left(\frac{\partial z}{\partial x}\right)^2 + \sigma_y^2 \left(\frac{\partial z}{\partial y}\right)^2 + 2\left(\frac{\partial z}{\partial x}\right)\left(\frac{\partial z}{\partial y}\right) COV(x, y) \qquad [32]$$

$$COV(x, y) = \sigma_x \, \sigma_y \, \rho(x, y) \qquad [33]$$

The first two terms in Eq. [32] represent the contribution of standard deviations of x and y to the standard deviation of the function z. The latter term represents the contribution of the correlation between x and y to the standard deviation of the function z. The term $COV(x,y)$ is the covariance of the variables x and y. The covariance of any two variables x and y is a function of their standard

deviations σ_x and σ_y, and of the coefficient of correlation between the two variables, $\rho(x,y)$, as shown in Eq. [33]. The same can be applied to any number of correlated and/or non-correlated variables. Applying the principles of error propagation to Eq. [5], the standard deviation of the curvature, σ_Ψ, can be estimated using the following expression.

$$\begin{aligned}\sigma_\Psi^2 = {} & \sigma_{I_e}^2 \left(\frac{\partial \Psi}{\partial I_e}\right)^2 + \sigma_{E_c}^2 \left(\frac{\partial \Psi}{\partial E_c}\right)^2 + \sigma_{M_s}^2 \left(\frac{\partial \Psi}{\partial M_s}\right)^2 + \\ & 2\left(\frac{\partial \Psi}{\partial I_e}\right)\left(\frac{\partial \Psi}{\partial E_c}\right) COV(I_e, E_c) + \\ & 2\left(\frac{\partial \Psi}{\partial E_c}\right)\left(\frac{\partial \Psi}{\partial M_s}\right) COV(E_c, M_s) + \\ & 2\left(\frac{\partial \Psi}{\partial I_e}\right)\left(\frac{\partial \Psi}{\partial M_s}\right) COV(I_e, M_s)\end{aligned} \quad [34]$$

M_s is the service moment. Note that M_s in the above equation and all of its correlated values will vanish since loading conditions are assumed to have no errors as discussed earlier. Therefore,

$$\sigma_\Psi^2 = \sigma_{I_e}^2 \left(\frac{\partial \Psi}{\partial I_e}\right)^2 + \sigma_{E_c}^2 \left(\frac{\partial \Psi}{\partial E_c}\right)^2 + 2\left(\frac{\partial \Psi}{\partial I_e}\right)\left(\frac{\partial \Psi}{\partial E_c}\right) COV(I_e, E_c) \quad [35]$$

where

$$\frac{\partial \Psi}{\partial I_e} = \frac{-M_s}{E_c\, I_e^2} \quad [36]$$

and

$$\frac{\partial \Psi}{\partial E_c} = \frac{-M_s}{E_c^2\, I_e} \quad [37]$$

To calculate the standard deviation of the effective moment of inertia, I_e, the principles of error propagation would have to be applied to Eq. [1] as follows

$$\sigma_{I_e}^2 = \sigma_{E_c}^2 \left(\frac{\partial I_e}{\partial E_c}\right)^2 + \sigma_{f_r}^2 \left(\frac{\partial I_e}{\partial f_r}\right)^2 + 2\left(\frac{\partial I_e}{\partial E_c}\right)\left(\frac{\partial I_e}{\partial f_r}\right) COV(E_c, f_r) \quad [38]$$

All other partial differentiations could be evaluated numerically by computer programs. The coefficients of correlation between the different

parameters discussed above can also be evaluated numerically if the values of these parameters are predicted using the appropriate prediction models.

It is important to note that in order to predict the value of the final curvature including long-term effects at any section along the member (e.g., Ψ_{Mid} in Eq. [4]), the same procedure outlined above would need to be applied for calculating the curvature three times. This is because the final curvature, Ψ_f, at any section is the sum of the long-term curvature due to sustained load, Ψ_t, as given in Eq. [29], and the live load curvature, Ψ_L. The live load curvature is calculated as the difference between the curvature due to dead and live loads, Ψ_a, and the dead load curvature, Ψ_d. i.e.,

$$\Psi_f = \Psi_t + \Psi_a - \Psi_d \qquad [39]$$

Therefore, the standard deviation of the final curvature at any section is a function of the standard deviations of the three stages Ψ_t, Ψ_a, and Ψ_d as shown in Eq. [40].

$$\begin{aligned}\sigma^2_{\Psi f} = {} & \sigma^2_{\Psi t}\left(\frac{\partial \Psi_f}{\partial \Psi_t}\right)^2 + \sigma^2_{\Psi a}\left(\frac{\partial \Psi_f}{\partial \Psi_a}\right)^2 + \sigma^2_{\Psi d}\left(\frac{\partial \Psi_f}{\partial \Psi_d}\right)^2 + \\ & 2\left(\frac{\partial \Psi_f}{\partial \Psi_t}\right)\left(\frac{\partial \Psi_f}{\partial \Psi_a}\right) COV(\Psi_t, \Psi_a) + \\ & 2\left(\frac{\partial \Psi_f}{\partial \Psi_a}\right)\left(\frac{\partial \Psi_f}{\partial \Psi_d}\right) COV(\Psi_a, \Psi_d) + \\ & 2\left(\frac{\partial \Psi_f}{\partial \Psi_t}\right)\left(\frac{\partial \Psi_f}{\partial \Psi_d}\right) COV(\Psi_t, \Psi_d)\end{aligned} \qquad [40]$$

Consequently, it can be seen that the effect of repeating the process three times to calculate the final curvature deflection, Ψ_f, is simply to accumulate further error in the final curvature value.

Knowing the final curvature and the curvatures due to shrinkage at the end supports, the deflection at mid-span can be evaluated as follows

$$\Delta = \frac{L^2}{96}\left(\Psi_{Left} + 10\Psi_f + \Psi_{Right}\right) \qquad [41]$$

For a simply-supported slab, Ψ_{Left} and Ψ_{Right} are induced by shrinkage alone. As Eq. [28] shows, shrinkage-induced curvature is not a function of the concrete properties. Therefore, the first and last derivatives of Eq. [41] will vanish, and the

standard deviation of the deflection, σ_{Δ}, will be directly proportional to the standard deviation of the final mid-span curvature, $\sigma_{\Psi f}$. Thus,

$$\sigma_{\Delta}^2 = \sigma_{\Psi_{Left}}^2 \left(\frac{\partial \Delta}{\partial \Psi_{Left}} \right)^2 + \sigma_{\Psi_f}^2 \left(\frac{\partial \Delta}{\partial \Psi_f} \right)^2 + \sigma_{\Psi_{Right}}^2 \left(\frac{\partial \Delta}{\partial \Psi_{Right}} \right)^2 \quad [42]$$

No correlation exists between the shrinkage-induced curvatures and the final curvature as the former depends only on the ratio of compression to tension reinforcement in the slab and the value of the shrinkage strain. Moreover, as the end curvature is not dependent on either the modulus of rupture or the modulus of elasticity, the standard deviations of the end curvature are zero, and the first and last terms in Eq. [42] vanish. The standard deviation of the deflection is then

$$\sigma_{\Delta} = \left(\frac{L^2}{9.6} \right) \sigma_{\psi_f} \quad [43]$$

EXAMINING THE EFFECT OF SOME PARAMETERS ON THE ERROR IN ESTIMATED DEFLECTIONS

By examining the above mathematical derivation, it can be seen that the two major parameters contributing to the standard deviation of the final deflection are the modulus of elasticity and the modulus of rupture, and their standard deviations. In addition, all the factors that affect the effective moment of inertia can also affect the standard deviation of the deflection (e.g., the magnitude of the creep coefficient, and the magnitude of the shrinkage strain).

A Mathcad® program was developed using the mathematical model presented above in Eq. [34] through Eq. [43] to predict the standard deviation of the calculated final deflection of a simply-supported, one-way slab. The standard deviations of the modulus of rupture and the modulus of elasticity are estimated by assuming a relative error, *RE*, in the mean value of the modulus of rupture, RE_{fr}, and a relative error in the mean value of the modulus of elasticity, RE_{Ec}, as shown in Eqs. [44] and [45], respectively.

$$\sigma_{f_r} = RE_{f_r} \cdot f_r \quad [44]$$

$$\sigma_{E_c} = RE_{E_c} \cdot E_c \quad [45]$$

The relative error in the parameters RE_{fr} and RE_{Ec} was assumed to range from 0 to 30 percent. When the effect of the level of error in the modulus of rupture was examined, a constant error in the modulus of elasticity of 5 percent

was assumed. Also when the effect of the change in the error in the modulus of elasticity was examined, a constant error in the modulus of rupture of 5 percent was assumed. Using these relative errors, the standard deviation of the modulus of rupture and the standard deviation of the modulus of elasticity were assumed, and then the standard deviation of the estimated deflection, σ_Δ, was evaluated. The relative error in the estimated deflection, RE_Δ, can be predicted using Eq. [46] in which Δ is the final deflection including the error.

$$RE_\Delta = \frac{\sigma_\Delta}{\Delta} \qquad [46]$$

Using the above procedure, a parametric study was carried out to examine the effect of a number of parameters on the error in the estimated deflection. These parameters included the concrete compressive strength, f_c', the mathematical model for predicting the modulus of rupture, f_r, the mathematical model for predicting the modulus of elasticity, E_c, the value of the shrinkage strain, ε_{sh}, the value of the creep coefficient, ϕ_c, and the sustained load ratio, q.

Case Study

A 40-MPa HPC, simply-supported, one-way slab is designed to span 4.5 m. The slab is 150-mm thick, and is reinforced with one layer of No. 5 bars spaced at 300 mm. This gives an equivalent reinforcement area of 667 mm^2 per m width. The bottom concrete cover to the reinforcement is 30 mm. The equivalent reinforcement ratio, ρ, is 0.0056. The slab is subjected to a superimposed dead load of 0.5 kPa and a live load of 2.4 kPa. The shrinkage strain, ε_{sh}, is 600 microstrains and the creep coefficient, ϕ_c, at the time of estimating the deflection is 2.0.

Using the ACI 318-99 U.S. customary units model (2), and for a concrete compressive strength of 40 MPa, the modulus of rupture and the modulus of elasticity will be 3.9 MPa and 29,915 MPa, respectively. The gross moment of inertia is 2.8×10^8 mm^4, while the cracked moment of inertia is 4.5×10^7 mm^4. The age-adjusted modulus of elasticity is 11,506 MPa.

Using this data, the shrinkage stress can be calculated as (Eq. [25])

$$f_{sh} = \left(\frac{3.5\,(0.0056)\,(1+0.8\,(2.0))\,(200\times10^3)}{29915 + 3\,(0.0056)\,(1+0.8\,(2.0))\,(200\times10^3)} \right) (11506)\,(600\times10^{-6}) \qquad [47]$$
$$= 1.8\ MPa$$

This shrinkage will reduce the cracking strength of concrete to 2.1 MPa (Eq. [24]) and, consequently, the cracking moment capacity to 7.9 kN.m. Due to the

omission of the compression reinforcement, the shrinkage will induce a curvature, Ψ_{sc}, at both ends of the slab. This curvature is calculated as follows (Eq. [28])

$$\Psi_{sc} = 0.7\left(\frac{600\times10^{-6}}{150}\right)\left(1-\frac{0}{667}\right) = 2.8\times10^{-6}\ mm^{-1} \quad [48]$$

The effective moments of inertia and the curvatures due to the different cases of loadings are summarized in Table 1. It is shown that the immediate deflection of the slab due to live load is 22.7 mm, and the estimated total deflection, Δ, including long-term deflection, is 25.1 mm. To evaluate the error in the estimated final deflection, Eqs. [34] to [43] would be applied. The coefficients of correlation between the different parameters incorporated in the covariance calculations for this case study were obtained by determining the values of these parameters as predicted using the ACI 318-99 model (2), and by considering concrete strengths in the range of 20 to 110 MPa.

The coefficients of correlation are presented in Table 2. Considering an error of 5 percent in both the modulus of rupture and the modulus of elasticity, the standard deviation of the estimated deflection, σ_Δ, is 2.8 mm, which represents a relative error in the estimated deflection, RE_Δ, of about 10 percent.

ANALYSIS AND DISCUSSION

To examine the effect of changing the concrete compressive strength on the relative error in the estimated deflection, two series of data were developed. In the first series, it was assumed that the relative error in the modulus of elasticity, RE_{Ec}, is fixed at 5 percent while the relative error in the modulus of rupture, RE_{fr}, varied between 0 to 30 percent. In the second series, RE_{fr} was assumed to be fixed at 5 percent while RE_{Ec} varied between 0 to 30 percent. The concrete strength in both series varied between 20 and 50 MPa. The results of the two series are presented in Figures 4 and 5, respectively.

Upon examining the two figures, it can be seen that a similar level of error in f_r and E_c will not yield the same level of error in the estimated deflection. For example, for an average error of 15 percent in f_r and an assumed error of 5 percent in E_c (Figure 4), the average error in the estimated deflection would be about 26 percent. For an average error of 15 percent in E_c and an assumed error of 5 percent in f_r (Figure 5), the average error in the estimated deflection would be about 20 percent. The relative error in the modulus of rupture, RE_{fr}, has a more pronounced effect on the relative error in the estimated deflection, RE_Δ, than the relative error in the modulus of elasticity, RE_{Ec}. This is because the contribution of the cracking moment and, consequently, the modulus of rupture to the effective

moment of inertia is much higher than the contribution of the modulus of elasticity.

Table 3 shows the standard deviations of the moments of inertia at the three different loadings (dead load, sustained load, and total load), the standard deviations of the final curvature, and the standard deviation of the final deflection for four different levels of assumed errors in f_r and E_c. It can also be noticed from Table 3, and Figures 4 and 5 that when RE_{Ec} is relatively small (e.g., between 0 and 5 percent) the relative error in the deflection, RE_{Δ}, will be lower than when RE_{Ec} is zero. This can be explained by considering the effect of the correlation between the parameters on the error accumulation. As can be noticed from Table 2, the effective moment of inertia and the modulus of elasticity are negatively correlated. This negative correlation would result in reducing the total error in the deflection when RE_{Ec} is relatively small. When RE_{Ec} is zero, the correlation contribution will be zero, and the relative error in the modulus of rupture, RE_{fr}, will govern the final value of the error in Δ.

The effect of shrinkage strain was also examined. Error analysis was repeated for the same case study and for a 40-MPa concrete compressive strength. The error in f_r ranged from 0 to 30 percent, while the error in E_c was assumed to be constant at 5 percent. The level of shrinkage strains ranged from 200 to 1000 microstrains. Figure 6 shows the effect of changing the shrinkage strain on RE_{Ec} due to the error in f_r. It can be noticed that the higher the shrinkage strain, the lower the final cracking strength, f_{cr}, (as in Eq. [24]) and consequently the lower the contribution of f_r to both the deflection and its error.

It is important to note that drawing general conclusions from this limited analysis is not the purpose of this paper. Other parameters that should be studied include the creep coefficient and the shrinkage strain. To account for the effect of the errors in these simultaneous parameters on the error in the computed deflection, the standard deviation of the curvature, σ_{Ψ}, should be evaluated using Eq. [49].

$$\sigma_{\Psi}^{\,2} = J\,C\,J^{T} \qquad [49]$$

where J is the matrix of derivatives and C is the matrix of variances given by Eqs. [50] and [51], respectively.

$$J = \left[\frac{\partial \Psi}{\partial M} \quad \frac{\partial \Psi}{\partial E_c} \quad \frac{\partial \Psi}{\partial f_{cr}} \quad \frac{\partial \Psi}{\partial \varepsilon_{sh}} \quad \frac{\partial \Psi}{\partial \varphi_c} \right] \qquad [50]$$

and

$$C = \begin{bmatrix} \sigma_M^2 & \sigma_M \sigma_{E_c} & \sigma_M \sigma_{f_{cr}} & \sigma_M \sigma_{\varepsilon_{sh}} & \sigma_M \sigma_{\phi_c} \\ & \sigma_{E_c}^2 & \sigma_{E_c} \sigma_{f_{cr}} & \sigma_{E_c} \sigma_{\varepsilon_{sh}} & \sigma_{E_c} \sigma_{\phi_c} \\ & & \sigma_{f_{cr}}^2 & \sigma_{f_{cr}} \sigma_{\varepsilon_{sh}} & \sigma_{f_{cr}} \sigma_{\phi_c} \\ & SYMMETRY & & \sigma_{\varepsilon_{sh}}^2 & \sigma_{\varepsilon_{sh}} \sigma_{\phi_c} \\ & & & & \sigma_{\phi_c}^2 \end{bmatrix} \quad [51]$$

Further investigation is currently underway using the above described approach to examine the effect of these parameters and their interdependence on the error in the computed deflection of reinforced concrete slabs.

SUMMARY

Prediction of immediate and long-term deflections is important in design of concrete members for satisfactory performance during their use. Design codes contain simplified procedures for predicting deflections that have proven to be inadequate in some situations, especially for deflection sensitive elements such as floor slabs. The calculated deflection is sometimes significantly less than the actual deflection causing serviceability problems. Because of the large number of uncertain parameters affecting the final deflection of a concrete member, it is difficult for designers to predict deflections with confidence.

This paper emphasized the importance of considering specific margins for the error anticipated in the calculated deflections of simply-supported, one-way reinforced concrete slabs. The paper examined the various sources of error associated with deflection calculation for these slabs. The theory of error propagation was applied to the mean curvature method of calculating deflections. A mathematical model was developed to be used for studying the effect of variation of concrete properties on the accuracy of the calculated deflections.

ACKNOWLEDGEMENTS

The authors would like to thank Mr. Pak Wong, P.Eng. and Mr. Paul Langohr, P.Eng., Stantec Consulting Ltd., and Dr. Naser El-Sheimy, the University of Calgary for their thoughtful comments and constructive criticism.

NOTATION

A_s	area of tension reinforcement
A_s'	area of compression reinforcement
b	width of compression face of a member
C	matrix of variances
$COV(x,y)$	covariance of variables x and y
d	distance from the extreme compression fibre to the centroid of tension reinforcement
E_a	age-adjusted modulus of elasticity of concrete
E_c	modulus of elasticity of concrete
E_s	modulus of elasticity of steel
f_c'	compressive strength of concrete
f_{cr}	cracking strength of concrete
f_{crack}	cracking strength of concrete (as used in CHBDC)
f_r	modulus of rupture of concrete
$f_{r\text{-}real}$	real modulus of rupture of concrete determined under site conditions
f_{sh}	internal tensile stress due to restrained shrinkage
f_t	mean tensile strength of concrete
h	overall depth of a member
i	index
I_{cr}	moment of inertia of a cracked section transformed to concrete, neglecting concrete in tension
I_e	effective moment of inertia
I_g	gross moment of inertia; moment of inertia of the gross concrete section about its centroidal axis neglecting reinforcement
J	matrix of derivatives
L	span length
M	bending moment
M_a	maximum moment in a member at the load stage deflection is calculated
M_{cr}	cracking moment
M_s	service moment
q	sustained load ratio
RE	relative error
RE_{Ec}	relative error in the mean value of the modulus of elasticity
RE_{fr}	relative error in the mean value of the modulus of rupture
RE_{Δ}	relative error in the estimated final deflection
S	time dependent factor used to calculate long-term deflections due to creep and shrinkage
t	any point in time
x	variable
y	variable
y_t	distance from the centroidal axis of gross concrete section to the extreme fibre in tension

z	variable
α	a term that accounts for the effect of cracking and the braking action of the reinforcement
Δ	final deflection at mid-span
Δ_{Mid}	mid-span deflection
ε_{sh}	shrinkage strain
ϕ_c	creep coefficient
γ	concrete density (in kg/m^3)
Γ	factor used in calculating shrinkage induced curvature
κ	a parameter that equals 0.85 to account for the initial plasticity of concrete when elastic analysis of the structure is to be performed
ρ	ratio of tension reinforcement
ρ'	ratio of compression reinforcement
$\rho(x,y)$	coefficient of correlation between two variables, x and y
σ	standard deviation
Ψ	curvature
Ψ_a	curvature due to dead and live loads
Ψ_d	curvature due to dead load
Ψ_f	final curvature at any section of an element
Ψ_i	initial curvature due to a sustained service moment
Ψ_L	curvature due to live load
Ψ_{Left}	curvature at the left end of a simply-supported slab
Ψ_{Mid}	curvature at mid-span of a simply-supported slab
Ψ_{Right}	curvature at the right end of a simply-supported slab
Ψ_{sc}	shrinkage induced curvature
Ψ_t	long-term curvature at any time t due to a sustained service moment
ζ	a multiplier used to estimate the additional long-term deflection due to creep and shrinkage

REFERENCES

1 Branson, D.E., Deformation of Concrete Structures, McGraw-Hill Book Co., New York, NY, 1977.

2 ACI Committee 318, Building Code Requirements for Structural Concrete (318-99) and commentary (318R-99), American Concrete Institute, Farmington Hills, MI, 1999.

3 CSA A23.3-M94 Technical Committee, Design of Concrete Structures, Canadian Standards Association, Toronto, Ontario, 1994.

4 Sherif, A.G. and Dilger, W.H., Analysis and Deflections of Reinforced Concrete Flat Slabs, Canadian Journal of Civil Engineering, Vol. 25, No. 3, June 1998, pp. 451-466.

5 Ghali, A. and Azarnejad, A., Deflection Prediction of Members of Any Concrete Strength, ACI Structural Journal, Vol. 96, No. 5, September-October 1999, pp. 807-816.

6 Gilbert, R.I., Deflection Calculation for Reinforced Concrete Structures – Why We Sometimes Get It Wrong, ACI Structural Journal, Vol. 96, No. 6, November-December 1999, pp. 1027-1032.

7 Gilbert, R.I., Shrinkage, Cracking and Deflection – the Serviceability of Concrete Structures, Electronic Journal of Structural Engineering (www.civag.unimelb.edu.au/ejse), Vol. 1, No. 1, 2001, pp. 15-37.

8 CEP-FIP Model Code 90, Model Code for Concrete Structures, Comité Euro-International du Béton (CEB) - Fédération Internationale de la Précontrainte (FIP), Thomas Telford Ltd., London, UK, 1993.

9 Ghali, A. and Favre, R., Concrete Structures: Stresses and Deformations, 2nd ed., E&FN SPON, London, UK, 1994.

10 Jokinen, E.P. and Scanlon, A., Field-Measured Two-Way Slab Deflections, Proceedings of the Annual Conference of the Canadian Society for Civil Engineering, Saskatoon, Saskatchewan, 1985, pp. 43-58.

11 Ghali, A., Elbadry, M., and Megally, S., Two-Year Deflections of the Confederation Bridge, Canadian Journal of Civil Engineering, Vol. 27, No. 6, December 2000, pp. 1139-1149.

12 Fling, R.S., Practical Considerations in Computing Deflection of Reinforced Concrete, Designing Concrete Structures for Serviceability and Safety, ACI SP-133, 1992, pp. 69-91.

13 Gardner, N.J., Design and Construction Interdependence, Concrete International, Vol. 12, No. 11, November 1990, pp. 32-38.

14 Frangopol, D.M., Probabilistic Design for Serviceability Related to Excessive Deformation, Proceedings of Symposium/Workshop on Serviceability of Buildings, National Research Council of Canada, Ottawa, Ontario, 1988, pp. 49-61.

15 Holicky, M., Fuzzy Concept of Serviceability Limit States, Proceedings of Symposium/Workshop on Serviceability of Buildings, National Research Council of Canada, Ottawa, Ontario, 1988, pp. 19-31.

16 Zundelevich, S., Hamada, H.S., and Chiu, A.N., Variability of Deflections of Simply Supported Precast Prestressed Concrete Beams, Deflection of Concrete Structures, ACI SP-43, 1974, pp. 547-571.

17 Thompson, D.P. and Scanlon, A., Minimum Thickness Requirements for Control of Two-Way Slab Deflections, ACI Structural Journal, Vol. 85, No. 1, January-February 1988, pp. 12-22.

18 Scanlon, A. and Pinheiro, L., Allowable Deflections: The Other Side of the Equation, Designing Concrete Structures for Serviceability and Safety, ACI SP-133, 1992, pp. 111-120.

19 Standards New Zealand NZS 3101, The Design of Concrete Structures, Standards New Zealand, Wellington, New Zealand, 1995.

20 Standards Australia AS 3600-1994, Concrete Structures, Standards Association of Australia, Homebush, Australia, 1994.

21 OHBDC, Ontario Highway Bridge Design Code, 3rd ed., Ministry of Transportation, Downsview, Ontario, 1992.

22 CHBDC, Canadian Highway Bridge Design Code, CAN/CSA-S6-00, CSA International, Rexdale, Ontario, 2000.

23 CHBDC-Commentary S6.1-00, Commentary on CAN/CSA-S6-00, CSA International, Rexdale, Ontario, 2001.

24 Carrasquillo, R.L., Nilson, A.H., and Slate, F.O., Properties of High-Strength Concrete Subjected to Short-Term Loads, ACI Journal, Vol. 78, No. 3, May-June 1981, pp. 171-178.

25 Raphael, J.M., Tensile Strength of Concrete, ACI Journal, Vo. 81, No. 2, March-April 1984, pp. 158-165.

26 Oluokun, F.A., Prediction of Concrete Tensile Strength from its Compressive Strength: An Evaluation of Existing Relations for Normal Weight Concrete, ACI Material Journal, Vol. 88, No. 3, May-June 1991, pp. 302-309.

27 Légeron, F. and Paultre, P., Prediction of Modulus of Rupture of Concrete, ACI Materials Journal, Vol. 97, No. 2, March-April 2000, pp.193-200.

28 Gardner, N.J., and Zhao, J.W., Creep and Shrinkage Revisited, ACI Materials Journal, Vol. 90, No. 3, May-June 1993, pp. 236-246.

29 Kovler, K., Drying Creep of Stress-Induced Shrinkage, Creep, Shrinkage and Durability Mechanics of Concrete and Other Quasi-Brittle Materials, Elsevier Science Ltd., 2001, pp. 67-72.

30 Bischoff, P.H., Effect of Shrinkage on Tension Stiffening and Cracking in Reinforced Concrete, Canadian Journal of Civil Engineering, Vol. 28, No. 3, June 2001, pp. 363-374.

31 Ghali, A., Deflection of Reinforced Concrete Members: A Critical Review, ACI Structural Journal, Vol. 90, No. 4, July-August 1993, pp. 364-373.

32 Manual of Concrete Practice, American Concrete Institute, Farmington Hills, MI, 2002.

33 Aïtcin, P.C., High-Performance Concrete, E&FN Spon, New York, NY, 1998.

34 Whiting, D.A., Detwiler, R.J., and Lagergren, E.S., Cracking Tendency and Drying Shrinkage of Silica Fume Concrete for Bridge Deck Applications, ACI Materials Journal, Vol. 97, No. 1, January-February 2000, pp. 71-77.

35 Shah, S.P., Swartz, S.E. and Ouyang, C., Fracture Mechanics of Concrete: Applications of Fracture Mechanics to Concrete, Rock and Other Quasi-Brittle Materials, John Wiley & Sons, Inc., New York, NY, 1995.

36 Baalabaki, W., Benmokrane, B., Chaallal, O., and Aïtcin, P.C., Influence of Coarse Aggregate on Elastic Properties of High-Performance Concrete, ACI Materials Journal, Vol. 88, No. 5, September-October 1991, pp. 499-503.

37 Dilger, W.H., and Wang, C., Shrinkage and Creep of High Performance Concrete (HPC) – A Critical Review, Adam Neville Symposium on Concrete Technology, Las Vegas, NV, June 1995, pp. 59-84.

38 Le Roy, R., de Larrard, F., and Pons, G., The AFREM Code Type Model for Creep and Shrinkage of High Performance Concrete, Fourth International Symposium on the Utilization of High Strength/High Performance Concrete, Proceedings−Vol. 1, Paris, France, May 1996, pp. 387-396.

39 Kennedy, J.B. and Neville, A.M., Basic Statistical Methods for Engineers and Scientists, Harper and Row Publishers, New York, NY, 1986.

SUGGESTED KEYWORDS

Deflection; modulus of rupture; serviceability; slab; theory of error propagation.

LIST OF TABLES

TABLES

Table 1 Mid-Span Effective Moments of Inertia, Curvatures, and Deflections for Different Loadings

Loading	M (kN.m)	I_e (mm^4)	Ψ (mm^{-1})	Δ (mm)
Dead	10.4	1.499×10^8	2.314×10^{-6}	---
Dead + Live	16.5	7.137×10^7	7.706×10^{-6}	---
Live	**6.1**	**---**	$\mathbf{5.392 \times 10^{-6}}$	**22.7**
Sustained	11.6	1.203×10^8	3.222×10^{-6}	---
Long-term	**---**	**---**	$\mathbf{1.125 \times 10^{-6}}$	**2.4**
Total	---	---	---	25.1

Table 2 Coefficients of Correlation Between the Different Parameters Incorporated in the Covariance Calculations

Correlated parameters	Coefficient of correlation
f_r and E_c	1.000
I_{es} (due to sustained moment) and E_c	-0.979
I_{ea} (due to total moment) and E_c	-0.980
I_{ed} (due to dead moment) and E_c	-0.980
Ψ_a (due to total moment) and Ψ_d (due to dead moment)	0.967
Ψ_a (due to total moment) and Ψ_s (due to sustained moment)	0.980
Ψ_s (due to sustained moment) and Ψ_d (due to dead moment)	0.998

Table 3 Standard Deviations of Moment of Inertia, Curvature, and Deflection at Mid-Span for Different Levels of Error in f_r and E_c

ER_{fr} ER_{Ec}	**0.05** **0.00**	**0.05** **0.05**	**0.10** **0.05**	**0.05** **0.10**
σ_{Ies} (mm^4)	2.096×10^7	1.752×10^7	3.848×10^7	1.407×10^7
σ_{Ied} (mm^4)	2.922×10^7	2.515×10^7	5.437×10^7	2.108×10^7
σ_{Iea} (mm^4)	0.733×10^7	0.492×10^7	1.225×10^7	0.249×10^7
$\sigma_{\Psi es}$ (1/mm)	5.614×10^{-7}	4.489×10^{-7}	9.847×10^{-7}	4.637×10^{-7}
$\sigma_{\Psi ed}$ (1/mm)	4.509×10^{-7}	3.642×10^{-7}	8.002×10^{-7}	3.536×10^{-7}
$\sigma_{\Psi ea}$ (1/mm)	7.917×10^{-7}	6.656×10^{-7}	13.140×10^{-7}	10.422×10^{-7}
σ_{Ψ} (1/mm)	16.230×10^{-7}	13.500×10^{-7}	27.354×10^{-7}	19.580×10^{-7}
σ_{Δ} (mm)	3.423	2.847	5.768	4.129

LIST OF FIGURES

FIGURES

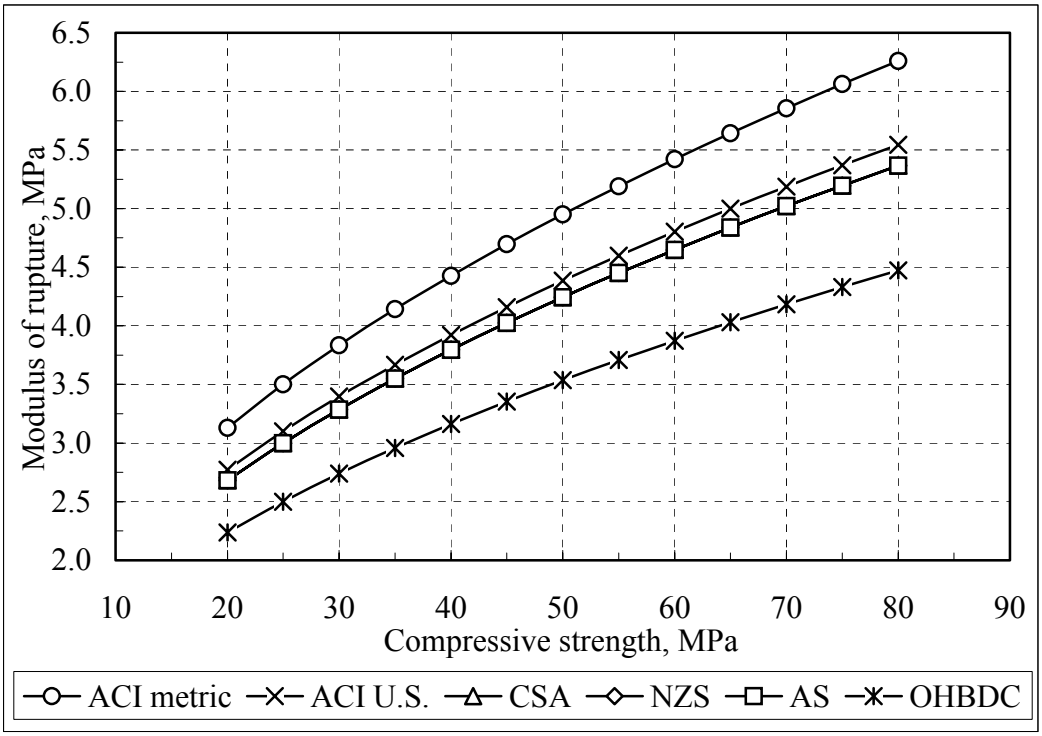

Figure 1 Comparison between modulus of rupture models in the different codes

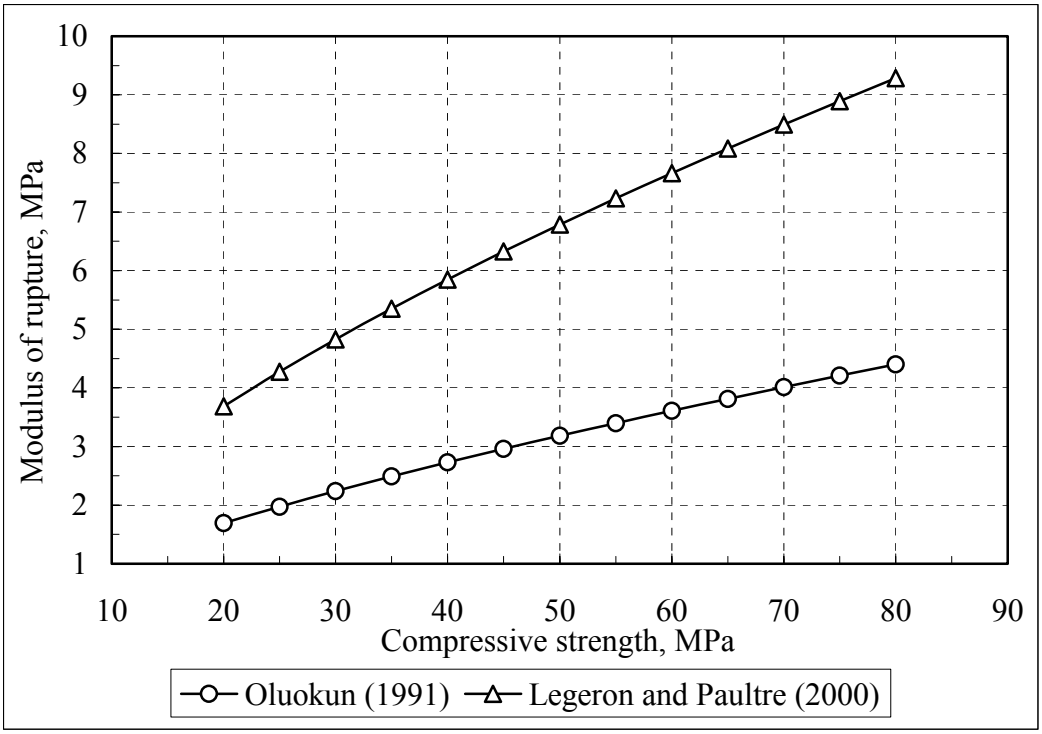

Figure 2 Comparison between modulus of rupture predicted by Eqs. [15] and [16]

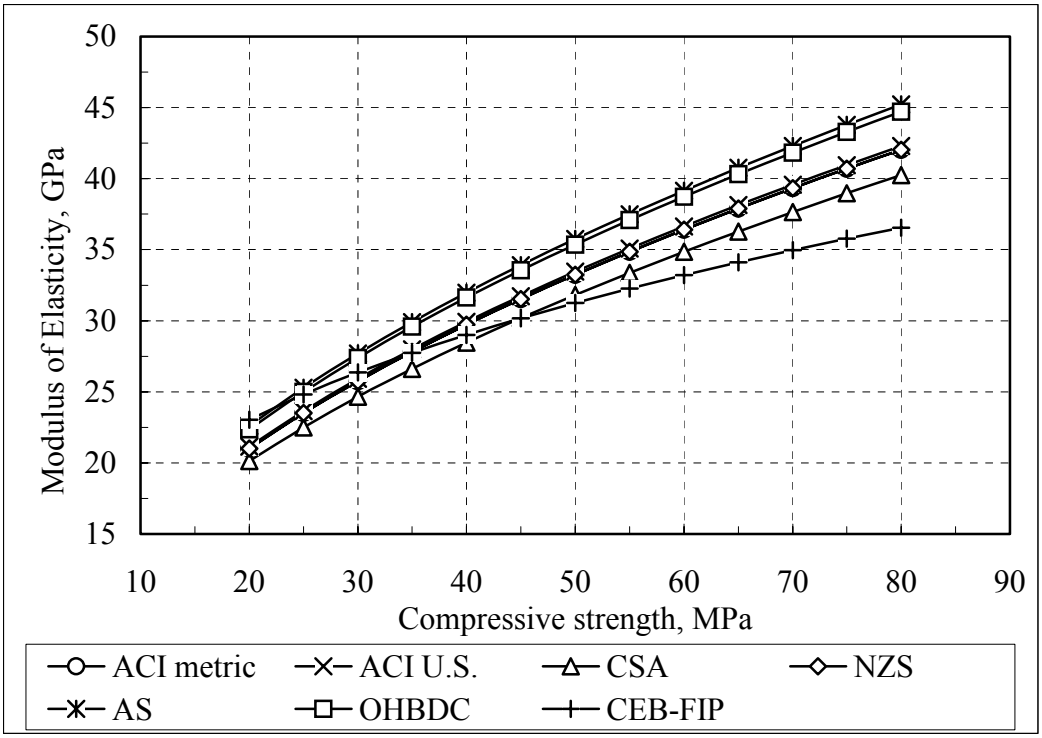

Figure 3 Comparison between modulus of elasticity models in the different codes

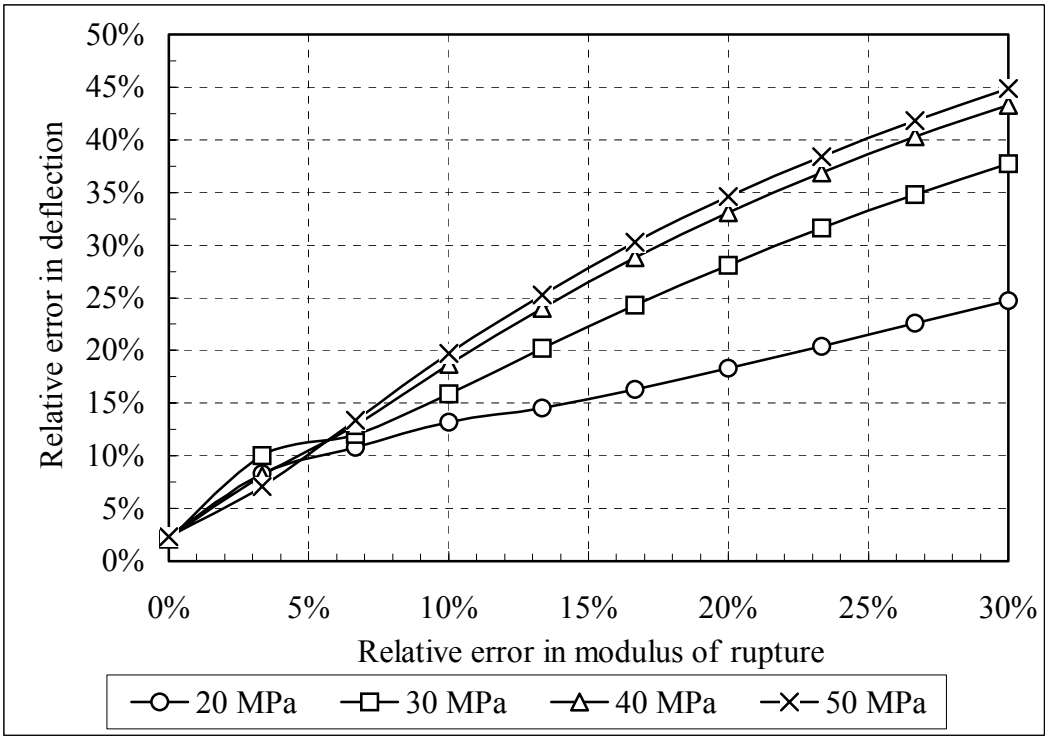

Figure 4 Effect of concrete strength on the error in the estimated deflection due to the error in the modulus of rupture (RE_{Ec} = 5%)

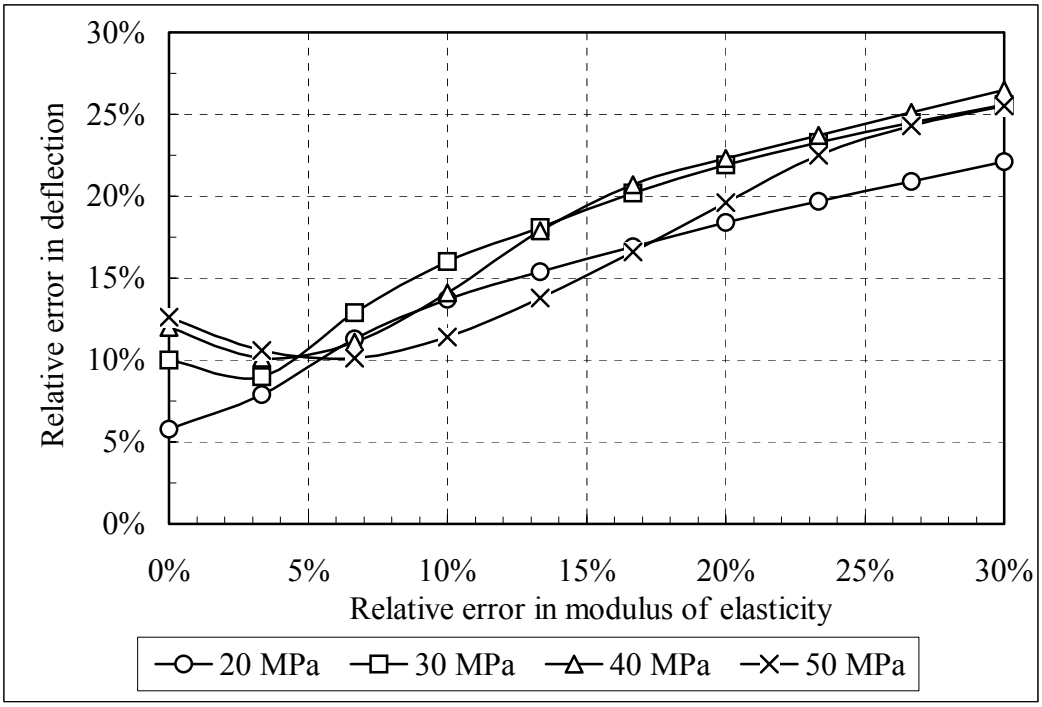

Figure 5 Effect of concrete strength on the error in the estimated deflection due to the error in the modulus of elasticity (RE_{fr} = 5%)

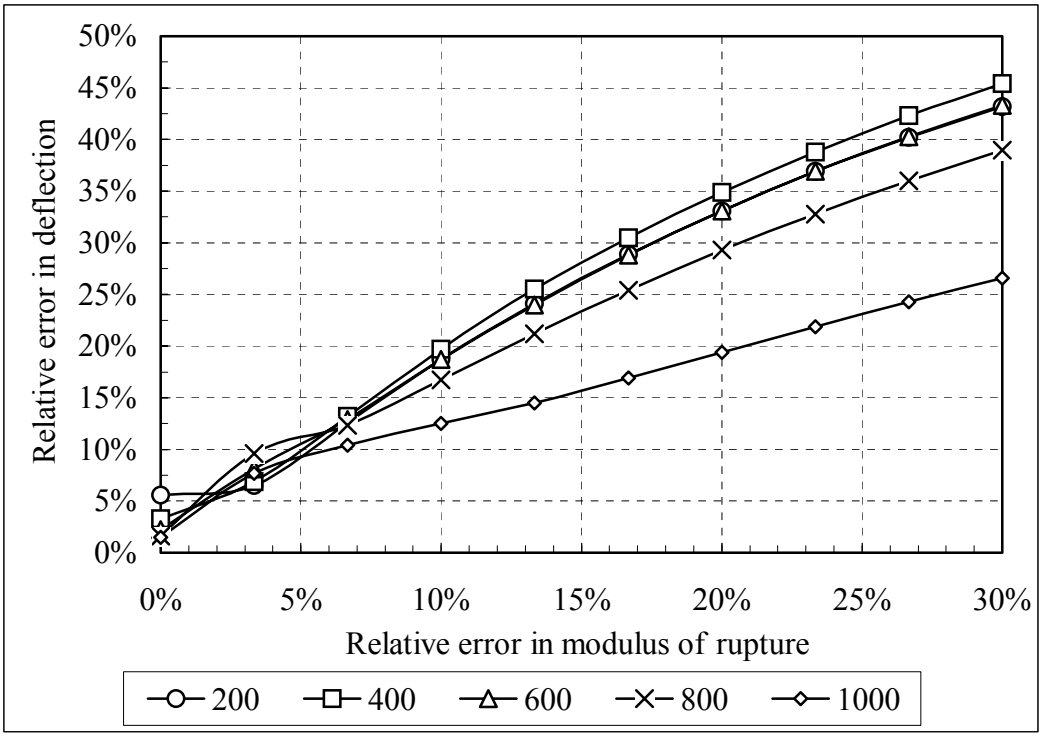

Figure 6 Effect of shrinkage strains on the error in the estimated deflection due to the error in the modulus of rupture (RE_{Ec} = 5%)